Simultaneous guidance of slow photons and slow acoustic phonons in silicon phoxonic crystal slabs

Vincent Laude, Jean-Charles Beugnot, Sarah Benchabane
Institut FEMTO-ST, Université de Franche-Comté, CNRS, Besançon, France
vincent.laude@femto-st.fr

Yan Pennec, Bahram Djafari-Rouhani
IEMN, Université de Lille 1, Villeneuve d'Ascq, France

Nikos Papanikolaou
Institute of Microelectronics, NCSR, Athens, Greece

Jose M. Escalante, Alejandro Martinez
Nanophotonics Technology Center, Universidad Politécnica de Valencia, Valencia, Spain

Abstract: We demonstrate theoretically that photons and acoustic phonons can be simultaneously guided and slowed down in specially designed nanostructures. Phoxonic crystal waveguides presenting simultaneous phononic and photonic band gaps were designed in perforated silicon membranes that can be conveniently obtained using silicon-on-insulator technology. Geometrical parameters for simultaneous photonic and phononic band gaps were first chosen for optical wavelengths around 1550 nm, based on the finite element analysis of a perfect phoxonic crystal of circular holes. A plain core waveguide was then defined, and simultaneous slow light and elastic guided modes were identified for some waveguide width. Joint guidance of light and elastic waves is predicted with group velocities as low as $c/25$ and 180 m/s, respectively.

OCIS codes: (160.5298) Photonic crystals, (130.5296) Photonic crystal waveguides, (160.1050) Acousto-optical materials, (350.7420) Waves.

References and links

1. J. Joannopoulos and J. Winn, *Photonic crystals: molding the flow of light* (Princeton Univ Pr, 2008).
2. M. S. Kushwaha, P. Halevi, L. Dobrzynski, and B. Djafari-Rouhani, "Acoustic band structure of periodic elastic composites," Phys. Rev. Lett. **71**, 2022–2025 (1993).
3. M. Maldovan and E. Thomas, "Simultaneous localization of photons and phonons in two-dimensional periodic structures," Appl. Phys. Lett. **88**, 251907 (2006).
4. M. Maldovan and E. Thomas, "Simultaneous complete elastic and electromagnetic band gaps in periodic structures," Appl. Phys. B: Lasers and Optics **83**, 595–600 (2006).
5. A. Akimov, Y. Tanaka, A. Pevtsov, S. Kaplan, V. Golubev, S. Tamura, D. Yakovlev, and M. Bayer, "Hypersonic modulation of light in three-dimensional photonic and phononic band-gap materials," Phys. Rev. Lett. **101**, 33902 (2008).
6. S. Sadat-Saleh, S. Benchabane, F. Baida, M. Bernal, and V. Laude, "Tailoring simultaneous photonic and phononic band gaps," J. Appl. Phys. **106**, 074912 (2009).
7. N. Papanikolaou, I. Psarobas, and N. Stefanou, "Absolute spectral gaps for infrared light and hypersound in three-dimensional metallodielectric phoxonic crystals," Appl. Phys. Lett. **96**, 231917 (2010).

8. S. Mohammadi, A. Eftekhar, A. Khelif, and A. Adibi, "Simultaneous two-dimensional phononic and photonic band gaps in opto-mechanical crystal slabs," Opt. Express **18**, 9164–9172 (2010).
9. Y. Pennec, B. Rouhani, E. El Boudouti, C. Li, Y. El Hassouani, J. Vasseur, N. Papanikolaou, S. Benchabane, V. Laude, and A. Martinez, "Simultaneous existence of phononic and photonic band gaps in periodic crystal slabs," Opt. Express **18**, 14301–14310 (2010).
10. A. Safavi-Naeini and O. Painter, "Design of optomechanical cavities and waveguides on a simultaneous bandgap phononic-photonic crystal slab," Opt. Express **18**, 14926–14943 (2010).
11. Y. El Hassouani, C. Li, Y. Pennec, E. H. El Boudouti, H. Larabi, A. Akjouj, O. Bou Matar, V. Laude, N. Papanikolaou, A. Martinez, and B. Djafari Rouhani, "Dual phononic and photonic band gaps in a periodic array of pillars deposited on a thin plate," Phys. Rev. B **82**, 155405 (2010).
12. A. Khelif, B. Aoubiza, S. Mohammadi, A. Adibi, and V. Laude, "Complete band gaps in two-dimensional phononic crystal slabs," Phys. Rev. E **74**, 046610 (2006).
13. M. I. Hussein, "Reduced bloch mode expansion for periodic media band structure calculations," Proceedings of the Royal Society A-Mathematical Physical and Engineering Sciences **465**, 2825–2848 (2009).
14. S. G. Johnson, S. Fan, P. R. Villeneuve, J. D. Joannopoulos, and L. A. Kolodziejski, "Guided modes in photonic crystal slabs," Phys. Rev. B **60**, 5751–5758 (1999).
15. J. Jin, *The finite element method in electromagnetics, Second edition* (Wiley, New York, 2002).
16. T. Xu, M. S. Wheeler, S. V. Nair, H. E. Ruda, M. Mojahedi, and J. S. Aitchison, "Highly confined mode above the light line in a two-dimensional photonic crystal slab," Appl. Phys. Lett. **93**, 241105 (2008).
17. V. Laude, Y. Achaoui, S. Benchabane, and A. Khelif, "Evanescent Bloch waves and the complex band structure of phononic crystals," Phys. Rev. B **80**, 092301 (2009).
18. V. Laude, A. Khelif, S. Benchabane, M. Wilm, T. Sylvestre, B. Kibler, A. Mussot, J. M. Dudley, and H. Maillotte, "Phononic band-gap guidance of acoustic modes in photonic crystal fibers," Phys. Rev. B **71**, 045107 (2005).
19. P. Dainese, P. Russell, N. Joly, J. Knight, G. Wiederhecker, H. Fragnito, V. Laude, and A. Khelif, "Stimulated Brillouin scattering from multi-GHz-guided acoustic phonons in nanostructured photonic crystal fibres," Nat. Phys. **2**, 388–392 (2006).

1. Introduction

The propagation of photons and acoustic phonons can be controlled separately by nanostructuration of the supporting materials. In particular, the introduction of periodicity leads to the photonic [1] and phononic [2] crystal concepts, respectively. Strong spatial confinement of the wave energy and reduction of group velocities by several orders of magnitude are made possible. In addition, periodic structures also allow one for tailoring the spatial dispersion of both photons and phonons, leading to non trivial effects such as negative refraction. It has to be noted that though the velocity of acoustic waves are five orders of magnitude lower than the velocity of light in a vacuum, it is the wavelength that governs the frequency ranges where waves strongly feel periodicity. Photonic crystals operating in the visible and near-IR spectrum, and phononic crystals operating in the GHz range have in common that the relevant wavelengths are in the sub-micron range.

Several combinations of materials and nanostructures have been suggested recently in order to obtain simultaneous photonic and phononic band gaps [3, 4, 5, 6, 7, 8, 9]. We term such artificial materials phoxonic crystals, but they are also termed opto-mechanical crystals by other authors [8]. 2D phoxonic crystal structures have been identified for silicon with air holes and silicon pillars in air [3, 4], and for lithium niobate with air holes [6]. 3D phoxonic crystals composed of metal spheres in a dielectric background have been proposed [7], but the dominant material platform is arguably the silicon slab perforated with periodic arrays of sub-micrometer holes [8, 10, 9] or supporting a periodic array of pillars [11]. Such nanostructures can be precisely manufactured using silicon-on-insulator (SOI) technologies. In the previous papers, the focus has mainly been on the identification of suitable parameters for the existence of simultaneous photonic and phononic band gaps. On the experimental side, efficient modulation of light pulses through Brillouin scattering by acoustic phonons has been observed for optical frequencies close to a photonic band edge [5].

In this paper, we aim at the theoretical demonstration that photons and acoustic phonons can be simultaneously guided and slowed down in specially designed nanostructures, via a phox-

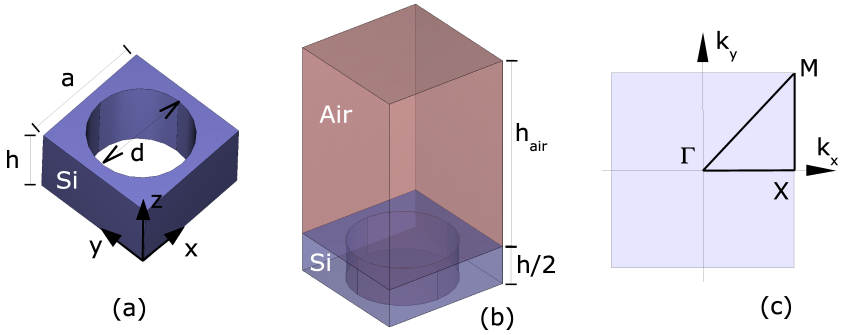

Fig. 1. Examples of unit-cells used in the analysis of phoxonic crystal slab structures. Two-dimensional periodic boundary conditions are applied at the lateral sides of the unit-cells. (a) For elastic waves, only the solid part (silicon) needs to be meshed. Traction-free boundary conditions are applied at the top and the bottom surfaces. (b) For photonic modes, the vacuum or air inside the holes and surrounding the slab needs to be taken into account. Free boundary conditions are applied at the top and the bottom surfaces of the air region, resulting in an artificial truncation of the computation domain. (c) First irreducible Brillouin zone showing the highest symmetry points.

onic band gap effect. The silicon phoxonic crystal slab geometry has been selected for its simplicity and potential ease of fabrication. Starting from known optimal geometrical parameters to obtain a complete phoxonic band gap [9], we investigate the dispersion of phoxonic crystal waveguides created by managing a line of defects in the periodic structure. The very strong spatial confinement created by the phoxonic band gap is found to be favorable for obtaining low group velocities for both sound and light waves.

2. Phoxonic crystal slab modes

A phoxonic crystal slab can be made by perforating periodically a thin membrane of a solid material (silicon in this work). Figure 1(a) depicts the unit-cell for computation of the dispersion relation and the modes of a phoxonic crystal slab. The basic geometrical parameters of such a structure are the thickness of the slab, h, the pitch of the array, a, and the diameter of the air holes, d. Fig. 1(c) shows the first irreducible Brillouin zone associated with the square lattice. The highest symmetry points Γ, X and M have wavevector coordinates $(0,0)$, $(\pi/a,0)$ and $(\pi/a,\pi/a)$, respectively.

Various numerical methods can be employed to compute the photonic and the phononic properties of periodic structures. We have in this work opted for the finite element method (FEM). In the phononic crystal slab case, FEM was recently shown to be highly efficient for obtaining band structures [12]. The FEM variational formulation for solid-air phononic crystals uses the three displacements as the dependent variables and 3D Lagrange finite elements. The practical advantage of FEM in the case of solids resides in the small size of the domain that has to be meshed. Indeed, only the solid part of the perforated silicon slab supports elastic waves and the free boundary conditions on the top and bottom faces yield perfect reflection of all elastic waves. There are at least two ways to obtain Bloch waves with FEM. One possibility is to introduce the Bloch-Floquet wavevector directly in the equations of propagation and thus in the variational formulation of the problem, together with symmetry boundary conditions for the lateral sides [13]. A second possibility is to use periodic boundary conditions for the lateral sides [12]. Both methods give exactly the same band structures but for numerical errors.

In the photonic case, there is an additional difficulty. Vacuum or air (with unit refractive

index) surrounds the silicon slab (with refractive index 3.6 at a wavelength in a vacuum of 1550 nm) and extends in principle to infinity. However, the computation domain has to be restricted to a finite region of space in practice. Since we are looking for eigenmodes of the system, the use of artificial boundary conditions such as perfectly matched layers (PML) is not adequate. We instead consider simple free boundary conditions a certain distance away from the slab surfaces. Consequently, waves radiated away from the slab can be reflected at the limits of the computation domain, and care has to be taken in the analysis of the obtained dispersion diagrams, in connection with the concept of the light line [14]. The light line is defined by the dispersion relation for light waves in a vacuum, $ck/\omega = 1$, with k the wavevector, ω the angular frequency, and c the speed of light in a vacuum. The light cone or radiative region is defined by $ck/\omega < 1$. Outside the light cone, any plane wave is necessarily evanescent and thus cannot radiate energy outside of the system. The air thickness is in practice adjusted so that evanescent waves have attenuated enough, so that the band structure for guided waves (lying outside the light cone) has converged. Inside the light cone, the artificial truncation of the air domain induces spurious bands, the number of which increases with the thickness of the air layer. No attempt was made at eliminating such spurious solutions from the photonic band structures reported in this paper, but this can be accomplished by examination of the energy distribution of each eigenmode, as illustrated later. Because of the symmetry of the slab structure with respect to the middle plane, it is further possible to separate photonic modes between even and odd. Even (respectively, odd) modes are also termed quasi-TE (resp., quasi-TM) modes. TE and TM here refer to the electric field vector being mostly transverse electric or magnetic, respectively. As a result of this symmetry property, only one half of the structure needs to be meshed, as shown in Fig. 1(b). The variational formulation for dielectric photonic crystals uses the magnetic field vector $\mathbf{H}$ as the dependent variable and 3D vector finite elements with vanishing divergence [15].

An exhaustive search for phoxonic crystal slab structures was conducted recently [9]. From these results, we have extracted the following configuration. First, the ratio of the slab thickness to the lattice constant, h/a, was found to be a key parameter for the existence of phoxonic band gaps. The value $h/a \approx 0.6$ was found to be an optimal one for the square lattice case. Second, phononic band gaps generally require large holes and the value $d/a = 0.86$ was selected. As we consider optical wavelengths around 1550 nm, the geometrical parameters used in this paper are precisely $a = 651$ nm, $h = 390$ nm, and $d = 560$ nm.

The phononic band structure is displayed in Fig. 2(a) and shows a complete elastic band gap appearing around 5 GHz, between the 6-th and the 7-th bands (8% relative band gap width). The first six Bloch modes at the M point of the first Brillouin zone are also shown for illustration in Fig. 2(b-g). It can be observed that none of these Bloch waves has a pure polarization, instead, their polarization has components along all three directions in space.

The photonic band structure is presented in Fig. 3(a). The dark gray region above the light line is the light cone for air; all waves having their dispersion represented by a point below the light line are guided by the phoxonic crystal slab. Two photonic band gaps for guided waves are found (appearing in white in Fig. 3(a)), around the reduced frequencies 0.35 and 0.42. The lower band gap is valid for even modes only, while the upper one is valid for both even and odd modes (i.e., is a complete band gap for guided waves). The first six even photonic modes are shown in Fig. 3(b-g) for the reduced wavevector value $k_x a/2\pi = k_y a/2\pi = 0.3$, somewhat midway along the ΓM direction. Only the first two even modes, Fig. 3(b-c), are outside the light cone and are thus certainly guided by the slab. However, even though it is apparent that the third, fourth and sixth modes are leaking in the surrounding air, the fifth mode is well guided inside the slab (Fig. 3(f)). From this observation, we can infer that a Bloch wave exhibing a dispersion lying within the light cone is only likely to be leaky; radiation to the surrounding air does not

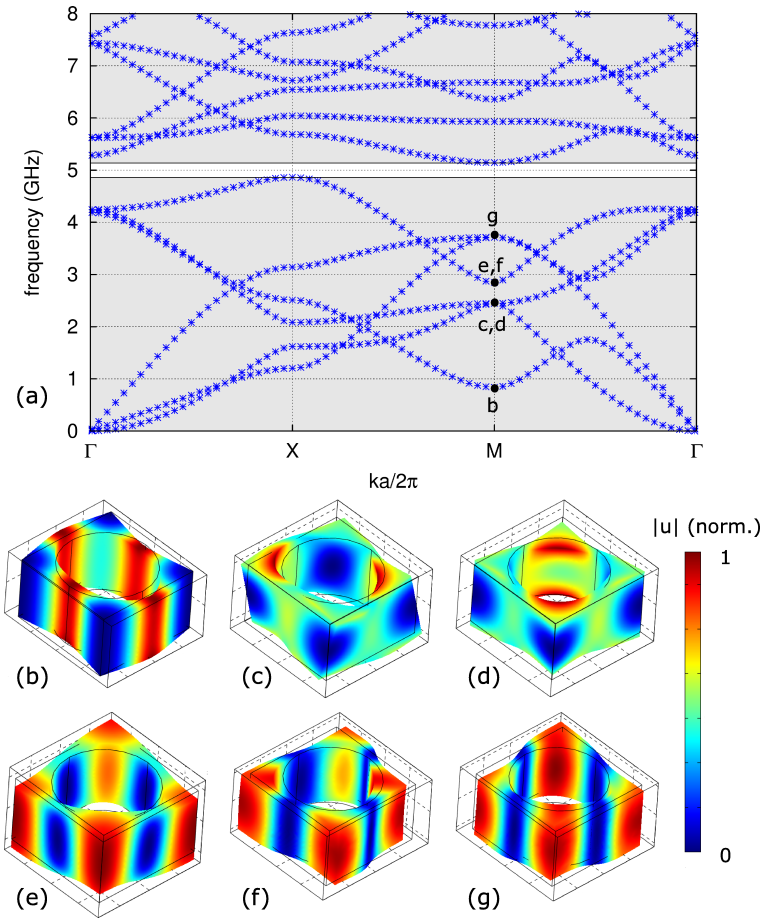

Fig. 2. (a) Phononic band structure for a periodic array of circular holes in a silicon slab with parameters $a = 651$ nm, $h = 390$ nm, and $r = 280$ nm. A complete band gap appears around 5 GHz. (b-g) Modal distribution of the displacements for the first six modes at the M point of the first Brillouin zone. The color bar is for the modulus of the total displacement while the deformation of the mesh is proportional to the algebraic displacements.

necessarily happens, as discussed by Xu *et al.* [16].

3. Guided slow phoxonic crystal slab modes

A phoxonic crystal waveguide was next defined by adding a solid core within the perfect crystal taken along the ΓX direction. Phononic and photonic Bloch modes are computed according to the super-cell technique, with the central solid core surrounded by three rows of phoxonic crystal along the Y direction, as depicted in Figure 4(a). As periodic boundary conditions are still applied along the Y direction, the simulated structure is actually an infinite array of straight cores separated by six rows of holes. However, all waves are evanescent in the hole array within a frequency band gap [17] and the separation of the cores is assumed to be sufficient to uncouple them. The waveguide width, w, was chosen equal to either a or $0.9a$. These values were chosen in order to center the phononic and photonic defect modes close to the center of the respective phononic and (lower) photonic band gaps.

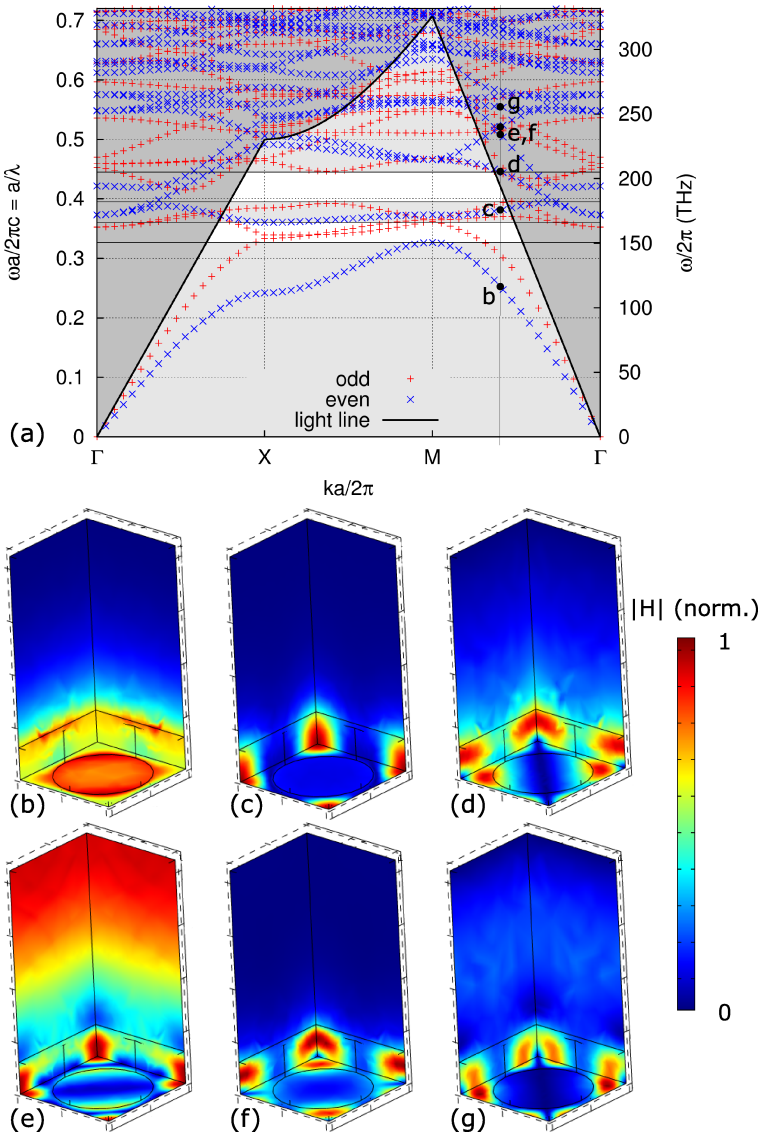

Fig. 3. (a) Photonic band structure for a periodic array of circular holes in a silicon slab with parameters $a = 651$ nm, $h = 390$ nm, and $r = 280$ nm. The left vertical axis is in units of the reduced frequency, $\omega a/2\pi c = a/\lambda$. The two photonic band gaps for guided waves appear in white. (b-g) Modal distribution of the modulus of the magnetic field vector $\mathbf{H}$ (a.u.) for the reduced wavevector value $k_x a/2\pi = k_y a/2\pi = 0.3$, somewhat midway along the ΓM direction, for the first six even modes.

Figs. 4(a-b) show the phononic band structure of the defect-based phoxonic crystal waveguide around 5 GHz. A total of up to four additional branches appear in the band gap region (indicated in white). Each of them supports a mode that is confined within the solid core by the phononic band gap effect. The most interesting of the four modes is the one with the flattest dispersion, appearing around 5 GHz for all axial wavevectors and shown as the continuous line in Fig. 4(b). The modal distributions of Bloch waves labelled (c), (d) and (e) are shown in

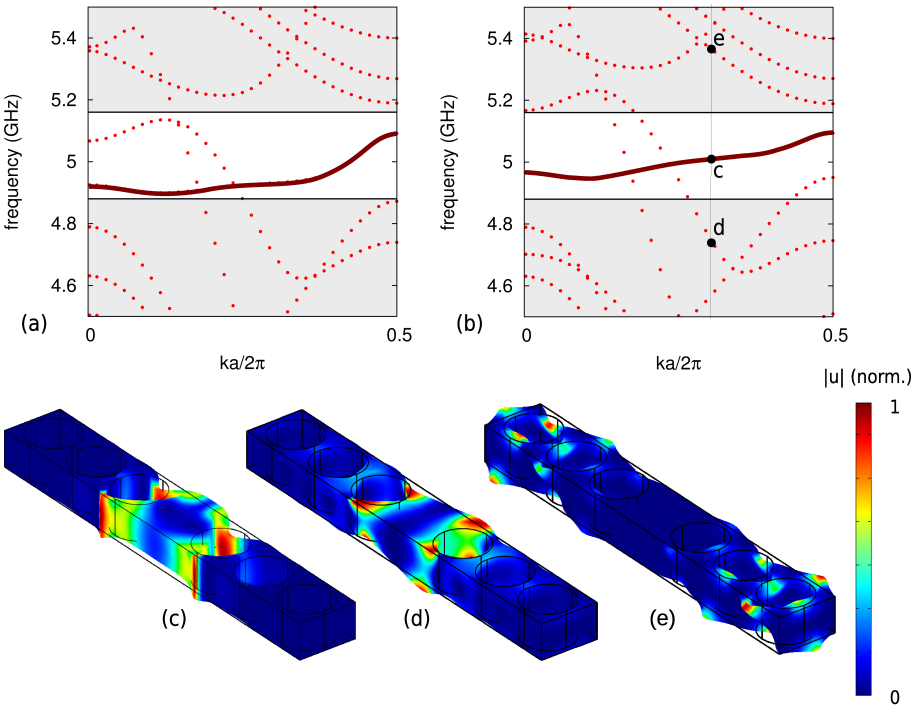

Fig. 4. Phononic band structure of a solid core phoxonic crystal waveguide defined along the ΓX direction in a square-lattice phoxonic crystal slab. In the supercell computation, three rows of holes surround a central solid core of width (a) $w = a$ and (b) $w = 0.9a$. The complete phononic band gap appears in white. The band supporting guided waves with the lowest group velocity is shown as a solid line. (c-e) Modal distributions of the displacements for three particular eigenmodes with $k_x a/2\pi = 0.3$. The color bar is for the modulus of the total displacement while the deformation of the mesh is proportional to the algebraic displacements.

Figs. 4(d-f), respectively, for the reduced wavevector value $k_x a/2\pi = 0.3$. Such plots allow us to check the effective guidance of the defect modes within the solid core. It must be noted that the polarization of these modes is again not pure, as it contains a mixture of shear horizontal, shear vertical, and longitudinal components. Bloch mode (c) is laterally guided by the phononic band gap effect for all wavevectors. Bloch mode (d) lies outside the phononic band gap but is also a defect mode; it is mostly guided by the core with some leakage to the side. It is however perfectly guided for $k_x a/2\pi < 0.25$. Bloch mode (e) also lies outside the phononic band gap but is a mode of the perfectly periodic crystal; it hence shows no lateral confinement at all.

Figure 5(a-b) shows the photonic band structure of the defect-based phoxonic crystal waveguide for even modes. The light cone appears as the dark gray region and the band gaps for guided Bloch waves appear in white. It can be seen that several defect modes are introduced and that their dispersion is quite sensitive to the value of the waveguide width, w. We are especially interested in the low band gap appearing in Fig. 5(b) around the reduced frequency 0.35, for $w = 0.9a$. In this forbidden frequency range, only one additional branch appears, with a very flat dispersion. The modal distributions of Bloch waves labelled (c) and (d) are shown in Figs. 5(c) and 5(d), respectively, for the reduced wavevector value $k_x a/2\pi = 0.45$. Both modes are laterally guided by the photonic band gap effect. The branch supporting mode (c) is

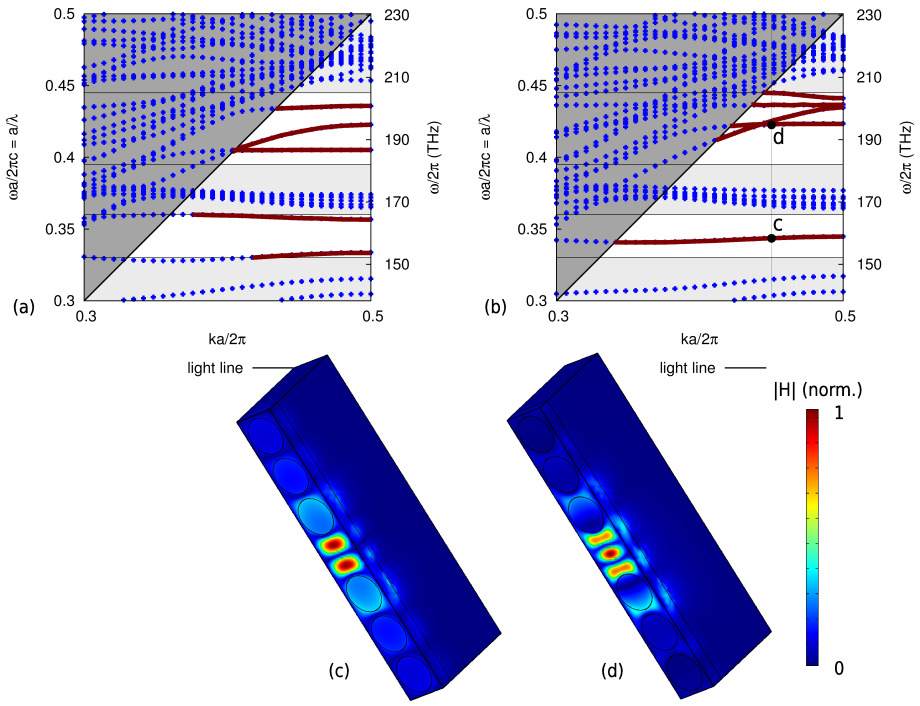

Fig. 5. Photonic band structure for waves in a solid core phoxonic crystal waveguide defined along the ΓX direction in a square-lattice phoxonic crystal slab. In the supercell computation, three rows of holes surround a central solid core of width (a) $w = a$ and (b) $w = 0.9a$. Two photonic band gaps for guided waves appear in white. The bands supporting waves latterally guided by the photonic band gap effect are shown with solid lines. (c-d) Modal distribution for two of these eigenmodes. The modulus of the magnetic field vector $\mathbf{H}$ is presented for the reduced wavevector value $k_x a/2\pi = 0.45$.

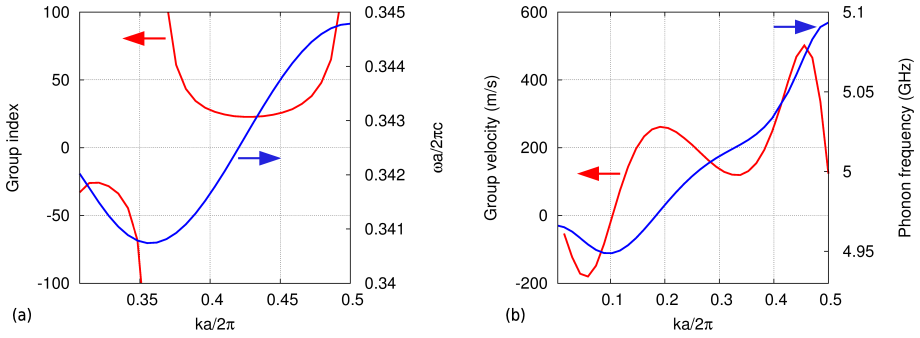

Fig. 6. (a) Dependence of the group index and of the reduced frequency with reduced wave vector, for the guided photonic mode labeled "c" in Fig. 5. (b) Dependence of the group velocity and of the frequency with reduced wave vector, for the guided phononic mode labeled "c" in Fig. 4.

especially interesting since the waveguide is monomode for even-polarized waves in this case.

The group velocity can be estimated from the band structures for guided waves from the definition $v_g = \frac{\partial \omega}{\partial k}$. In the phononic case, it is customary to consider the group index defined by

$n_g = c/v_g$. Figure 6(a) displays the dependence of the group index with reduced wave vector for the guided photonic mode labeled "c" in Fig. 5. It can be seen that this quantity can be either positive or negative, depending on the wave vector. However, from an experimental point of view, the most useful part of the spectrum is arguably found around the reduced frequency $\omega a/2\pi c = 0.343$, where the group index remains approximately constant ($n_g \approx 25$). Fig. 6(b) shows the dependence of the group velocity with reduced wave vector, for the guided phononic mode labeled "c" in Fig. 4. Around the 5 GHz phonon frequency, the group velocity varies around a mean value of 180 m/s, more than 30 times less than the speed of any bulk wave in silicon and less than the speed of sound in air.

4. Conclusion

We have presented the principle of a phoxonic crystal slab waveguide managed by inserting a linear solid core defect in a nanostructured silicon slab presenting simultaneously a phononic and a photonic band gap. Such a nanostructure can be conveniently obtained using silicon-on-insulator technology. Geometrical parameters for simultaneous photonic and phononic band gaps were first chosen, based on the finite element analysis of a perfect phoxonic crystal of circular holes. A plain core waveguide was then introduced, and simultaneous guidance of slow photons and slow acoustic phonons was identified. Optical and acoustic group velocities as small as $c/25$ and 180 m/s over a usable frequency range were predicted, respectively. The structure of the proposed phoxonic crystal slab waveguide is markedly different from the optomechanical waveguide structures proposed by Safavi *et al.* [10]. The former structures were designed to optimize the optomechanical interaction, where coupling of photons and phonons would be provided by the periodic motion of the boundaries. In contrast, the phoxonic crystal waveguides we have presented guide photons and phonons in a small central solid core, and are thus better suited to situations where acousto-optical coupling is provided by the elasto-optical effect. As such, they bear an analogy to photonic crystal fibers which were shown to support the joint guidance of photons and phonons [18, 19]. A difference is that the periodic nanostructuration in the plane of the slab makes it possible to tailor slow wave propagation, which is less easy when the 2D structuration runs along the core of a photonic crystal fiber.

Acknowledgment

This research has received funding from the European Community's Seventh Framework Programme (FP7/2007-2013) under grant agreement number 233883 (TAILPHOX).